



Review

<https://doi.org/10.1631/jzus.A2400015>



High-performance and multifunctional organic photovoltaic devices

Yiming WANG¹, Lijian ZUO^{1,2}✉

¹State Key Laboratory of Silicon Materials, Department of Polymer Science and Engineering, Zhejiang University, Hangzhou 310027, China

²Zhejiang University-Hangzhou Global Scientific and Technological Innovation Center, Hangzhou 310014, China

Abstract: Organic photovoltaic devices (OPVs) are emerging as a promising renewable energy source for the future. Their unique advantages, such as semitransparency, light weight, superior flexibility, and low cost, enable a wide range of applications. However, compared to silicon-based photovoltaics, OPVs still face challenges for further improving their efficiency. Additionally, there is a need to explore their potential of multi-functionality for practical application in various scenarios. This review summarizes the recent achievements in optimizing device performance and enhancing power-conversion efficiency, particularly via tuning the intermolecular interaction to reduce the electron-vibration coupling and non-radiative charge recombination (denoted as the “dilution effect”). Moreover, the representative development of ultra-thin Ag transparent electrode-based OPVs with multi-functional capabilities (such as semitransparency, flexibility, stretchability, and better aesthetics) has also been covered. Therefore, this review aims to provide a broad landscape on the recent development of OPV and to unlock the full potential of OPVs.

Key words: Organic photovoltaic; Multi-component; Semitransparent; Flexibility

1 Introduction

Reducing global energy consumption from fossil fuels requires innovative and cost-effective renewable energy technologies. Photovoltaics (PVs) can fulfil this need amply if deployed over a large enough area (Maka and Alabid, 2022). As a result, terrestrial PV technology has emerged as the most rapidly growing electrical energy source in the past decade, and now accounts for ~6% of the total electrical supply in China (Victoria et al., 2021; Zhang ZX et al., 2023). No doubt, this will continue soaring. Installing more PV panels in remote and sunny regions could theoretically meet the growing demand for energy, but implementation is restricted by several practical factors (Zhong et al., 2022; Zhang HT et al., 2023; Zhang ZX et al., 2023). First, the area suitable for PV plants is limited in most energy-demanding countries. Second, the maintenance and distribution costs, as well as adverse environmental effects, make numerous plants less practical. Third,

the traditional structure of energy conveyance and consumption requires averting the direct current into alternating current, transportation along grids, and conversion to direct current for most household appliances. This process sacrifices a considerable proportion of the energy produced. In addition, the energy generated by PV panels needs to be conserved in the daytime and released at night. These drawbacks make terrestrial PV-based electrical systems less efficient.

One approach to tackling these issues is through developing PV technology that can be installed near homes for instant use. This can be achieved by integrating PV panels with surfaces used in daily life, e.g. vehicles, buildings, clothing, and wearable electronics, in ways that will not greatly impact function or aesthetics. Applications in outer space are also a possibility. Organic photovoltaic devices (OPVs) based on highly conjugated conductive polymers exhibit inherent stability against high radiation doses, and the excellent photovoltaic performance retention of OPVs when operating at high-altitude platform stations makes them promising for applications in outer space (Kumar et al., 2010; Datt et al., 2022). To further advance the sustainability of photovoltaic technology, ongoing research on and enhancements in device design and performance are essential. Future endeavors in photovoltaic

✉ Lijian ZUO, zjuzlj@zju.edu.cn

Lijian ZUO, <https://orcid.org/0000-0003-0338-1198>

Received Jan. 10, 2024; Revision accepted Mar. 18, 2024;
Crosschecked May 20, 2024; Online first June 14, 2024

© Zhejiang University Press 2024

technology will strive to enhance functionality, including features like semi-transparency, flexibility, and aesthetics, to seamlessly integrate solar power into our everyday lives (Tak et al., 2017; Traverse et al., 2017; Liu et al., 2022; Huang et al., 2023). In this context, organic semiconductor-based PVs have a unique advantage, due to their intrinsic optoelectronic and processing properties. For example, the organic semiconductor has a distinct absorption profile, which makes it a rare but valuable candidate for achieving selective absorption for semitransparent PV application. The organic semiconductor is also famous for its flexibility and stretchability in device applications, which further widens its applicability in curved structures and dynamically flexible and stretchable applications. Furthermore, organic semiconductors can be manufactured in vivid colors for aesthetic applications.

Currently, the relatively low device efficiency they offer is still the major obstacle for the practical application of OPVs. Their intrinsic limitations include high exciton-binding energy, short exciton-diffusion distance, and severe non-radiative charge recombination (Veldman et al., 2008; Yuan et al., 2011). The innovation of donor:acceptor (D:A) heterojunction structure and bulk-heterojunction structure successfully compensates for the high exciton-binding energy and short exciton-diffusion length, and enables efficient charge generation. As a result, high photon-to-electron conversion efficiency was achieved by Park et al. (2009), with internal quantum efficiency around 100%. As shown in Table 1, it is clear that specific device parameters, i.e. the external quantum efficiency (EQE) and the fill factor (FF), are quite similar to those of inorganic counterparts. However, the open-circuit voltage (V_{oc}) loss is still large, which has become the most critical challenge in device efficiency. It has been generally recognized that this severe V_{oc} loss is caused by

non-radiative charge recombination (Vandewal et al., 2009). As a matter of fact, the non-radiative decay process occurs throughout the whole photon-to-electron process: (1) The exciton generated upon light incidence is quenched via thermal relaxation. (2) The subsequent exciton separation results in a low-energy charge-transfer (CT) state, which is regarded as the dominant species for non-radiative charge recombination (according to the energy-gap law). (3) Following CT separation, polarons will form and ultimately be collected by an electrode to drive the out-circuit appliance. Meanwhile, a charge back-transfer process will occur and cause triplet states, which will be quenched to ground state via the non-radiative mode. Vandewal et al. (2009) systematically studied the electron-vibration coupling in fullerene-based OPVs, and pessimistically concluded that the intrinsic electron-vibration coupling from the backbone of the active layers inevitably induces large non-radiative charge recombination and subsequent large V_{oc} loss (Benduhn et al., 2017). This sets an upper efficiency limit of 25.5% for OPVs. By comparison, the efficiency limit for a normal PV technique is over 33% (according to the Shockley-Queisser limit) when no non-radiative charge recombination occurs. Moreover, electron-vibration coupling is also significantly involved in the CT state's induced non-radiative charge recombination. Most high-performance OPVs are currently fabricated on glass/indium tin oxide (ITO) substrates with an opaque metal film as the back electrode. This structure offers a good compromise between transparency and conductance. However, it also results in rigid, expensive, fragile, non-transparent, and heavy devices. Consequently, it diminishes many of the usual advantages of OPVs, such as intrinsic flexibility, vibrant color, light weight, and cost-effectiveness (Zhao et al., 2022; Zheng et al., 2022). Developing more advanced device structures and non-active materials like interfacial layers and electrodes is necessary to fully explore the potential of OPVs. For instance, achieving superior flexible or stretchable OPVs requires the development of appropriate device structures, transparent electrodes, back electrodes, substrates, and interfacial layers. One notable feature of organic semiconductors for multi-functional photovoltaic applications is their selective absorption profiles. They strongly absorb near-infrared light, while allowing penetration of most visible photons. This characteristic sufficiently enables integration with windows, allowing simultaneous electricity

Table 1 Device parameters of different single-junction PVs (Zuo et al., 2022)

Item	E_g (eV)	V_{oc} (V)	FF (%)	V_{oc} loss (V)	EQE (avg.) (%)
GaAs	1.43	1.10	>85	0.33	>95
Si	1.11	0.75	~85	0.36	>95
CdTe	1.44	1.01	>80	0.43	>90
CIGS	1.12	0.74	>80	0.38	>90
OPV	1.52	0.88	<80	0.56	<80

E_g : energy gap; CIGS: copper indium gallium selenide

generation without compromising window functionality (Tak et al., 2017; Wang et al., 2021). Additionally, it facilitates heat control of the building by managing middle-infrared photons (Amirkhani et al., 2019). However, high-performance semi-transparent OPVs require management of optical properties throughout the entire device to maximize selective absorption.

In this review, we summarize the recent work to address electron-vibration-induced non-radiative charge-recombination loss via the dilution effect (or the phenomenon of intermolecular influence on the electron-vibration coupling) for high device performance, as well as the new concepts and device structures targeted to various applications of OPVs. These understandings and strategies essentially enable the progress of high-performance OPVs with certified efficiency approaching 20%, which is currently the best result of single-junction OPVs. These new device structures, including semitransparent and flexible/stretchable structures, also represent the best compromise between device performance and functionality.

2 Effects of electron-vibration coupling

Electron-vibration coupling is regarded as one of the most important channels for non-radiative charge recombination, as reported in our previous work (Zuo et al., 2022). Since this coupling originates from the conjugated backbones of an organic semiconductor, the resultant V_{oc} loss appears to be unavoidable and severe. However, it should be noted that electron-vibration coupling is also intimately linked to the intermolecular interactions/environment, where two major effects, i.e., local polarization and molecular packing, are involved.

2.1 Polarization effect

The excited state of a molecule typically exhibits a larger dipole moment compared to the ground state. The coulombic interactions that occur in excited states cause dramatic change in the surroundings. Therefore, the local surrounding polarizability also becomes involved; the change in the surrounding chemical environment contributes to electron-vibration couplings. A prominent phenomenon in this mechanism is the solvation effect, in which the solute molecules dissolved in solvents with different dipole moments tend to exhibit different optical spectra (Bulović et al., 1998, 1999).

It is generally observed that the absorption and photoluminescence (PL) spectra exhibit an obvious red shift with higher solvent polarity, while the PL quantum efficiency (PLQY) tends to decrease. A similar effect has been observed in the solid state, and is termed the “solid-state-solvation” effect. It is generally adopted as an effective method to tune the excitonic and optical properties of organic semiconductors in thin films (Northey et al., 2017). Usually, dispersing the emitter or dopant in a continuous matrix of a semiconducting material with a larger band gap significantly suppresses non-radiative charge recombination and induces higher luminescence. As a result, the solid-state-solvation effect has been widely explored in organic light-emitting devices (OLEDs), and demonstrated to be an important strategy to achieve high performance. Although the working mechanism for the suppressed non-radiative charge recombination underlying the solid-state-solvation effect is complicated for OLED applications, the change in surrounding polarizability certainly plays a role. This role becomes even more important for OPVs, because the dipole moment for OPV materials is even larger. To absorb more photons in the solar spectra, OPV materials must have a much lower band gap (optimal $E_g \approx 1.30$ eV from the Shockley–Queisser (S-Q) limit) than OLED materials (visible region of about 1.77–3.10 eV). To achieve a lower band gap, one of the most frequently used strategies is the donor-acceptor alternating strategy, and the internal charge transfer is closely linked to band gap size. The stronger the intramolecular charge transfer (ICT), the lower the band gap (Lim et al., 2021; Scharber and Sariciftci, 2021). Therefore, the classic OPV materials typically exhibit larger conjugation and stronger polarity. This affects the properties of the excited states as well as electron-phonon coupling. Because the photon absorption of organic molecules induces an excited state of a larger dipole moment, it will further induce the change of surrounding molecules. This also relaxes the energy of the excited state, corresponding to the coordinate shift in the overall system.

2.2 Molecular packing effect

Vibration of chemical bonds is the most important factor in electron-vibration coupling, particularly for bonds that directly contribute to the molecular frontier orbitals. Bond vibration can also be directly affected by molecular packing. For example, in solution, free rotation of the phenyl ring of tetraphenylethylene (TPE)

occurs, while this motion is suppressed in a solid state, contributing to the famous aggregation-induced emission (AIE) (Hong et al., 2009, 2011). Furthermore, the different molecular aggregations, e.g. the H- and J-aggregates, can also affect electron-vibration coupling dramatically. Amorphous and crystalline packing structures affect electron-vibration coupling as well. These findings indicate that it is possible to take advantage of the intermolecular effect to suppress electron-vibration coupling and the corresponding non-radiative charge recombination.

3 Dilution effect for multi-component OPVs

The most popular device structure for OPVs is the bulk-heterojunction (BHJ), which contains a nanoscale phase-separated continuous interpenetrating network of donor and acceptor binary blend (Huang et al., 2014). This structure successfully compensates for the high exciton-binding energy and poor ambipolar charge transport of OPV materials, and thus enables high photocurrent generation and collection efficiency, corresponding to a high external quantum efficiency of over 90% and a high FF of over 0.8. In order to tailor the intermolecular interaction for electron-vibration coupling and non-radiative charge-recombination suppression, the most intuitive method is to incorporate a third component to form a multi-component blend, e.g. the ternary structure. In fact, the ternary has long been proposed for different purposes, such as achieving complementary absorption, optimizing morphology, and facilitating charge transfer. Different working mechanisms of the ternary blend have also been proposed, e.g. the charge-transfer model, energy-transfer model, parallel model, and alloy model (Günther et al., 2023; Wang et al., 2023). Further, the uncertainty in terms of fundamental understanding of multi-component OPVs has hindered the development of a unified material selection rule to universally achieve higher device performance. In most ternary OPVs, lower non-radiative charge recombination and blue-shift in absorption spectra have been generally observed, while the fundamental mechanism underlying these phenomena is less explored.

3.1 Proof-to-concept study

We took advantage of the ternary strategy for a novel approach to tailoring the electron-vibration

coupling in OPVs via controlling the intermolecular interaction, and proposed using the dilution effect for multi-component OPVs. By blending two non-fullerene acceptors (NFA), specifically ITIC and 4TIC, we found the two molecules formed a good mixture at the molecular level, as shown in Fig. 1 (Zuo et al., 2022). Interestingly, the blend film exhibited a steeper absorption tail, indicating the formation of “ordered” intermixing. Moreover, we identified that the photon-emission center was still localized on the low-band gap 4TIC, and the Forster energy transfer from ITIC and 4TIC occurred in the blend. However, ITIC provided a lower local polarizability surrounding 4TIC and interrupted the molecular packing of 4TIC. As a result, the emission properties of the blend were quite different from those of pristine 4TIC; the PL spectra exhibited a blue shift and PLQY increased. We also numerically analyzed the electron-phonon coupling, and calculated the Huang-Rhys parameter (S_{H}) for 4TIC in pristine and blend films, by decoupling the Barry-center and Stokes shift from the absorption and PL spectra. We found that the S_{H} of 4TIC in the blend was reduced, and this unambiguously verified that electron-vibration coupling was suppressed via the intermolecular interactions. Further, from the analytical model based on the Marcus-transition theory and Frank-Condon equations, we identified that the degree of S_{H} suppression exactly accounted for the four-fold increase in PLQY (de Jong et al., 2015). We then analyzed the electron-vibration coupling in the device via the EQE and electroluminescence (EL) spectra, and found that the properties of the blend film were passed on to the device, contributing to the increase in the electroluminescence quantum efficiency (ELQE).

For an OPV device, charge generation and transport are also very important. Our comprehensive analysis showed that the dilution effect does not negatively affect the charge-generation process, but the incorporation of ITIC becomes a bridge for electron transfer from the PBDB-T donor to the 4TIC acceptor. Interestingly, we observed that the charge could spontaneously jump from 4TIC to ITIC, which is supposed to be a thermally-activated process (Shi et al., 2017; Liu et al., 2018). We identified this mechanism using several NFA pairs of the different lowest unoccupied molecular orbital (LUMO) offsets, and found the intensity of the higher LUMO NFAs to be in inverse proportion to LUMO offsets. This significantly affected the charge-transport process, because the microscopic

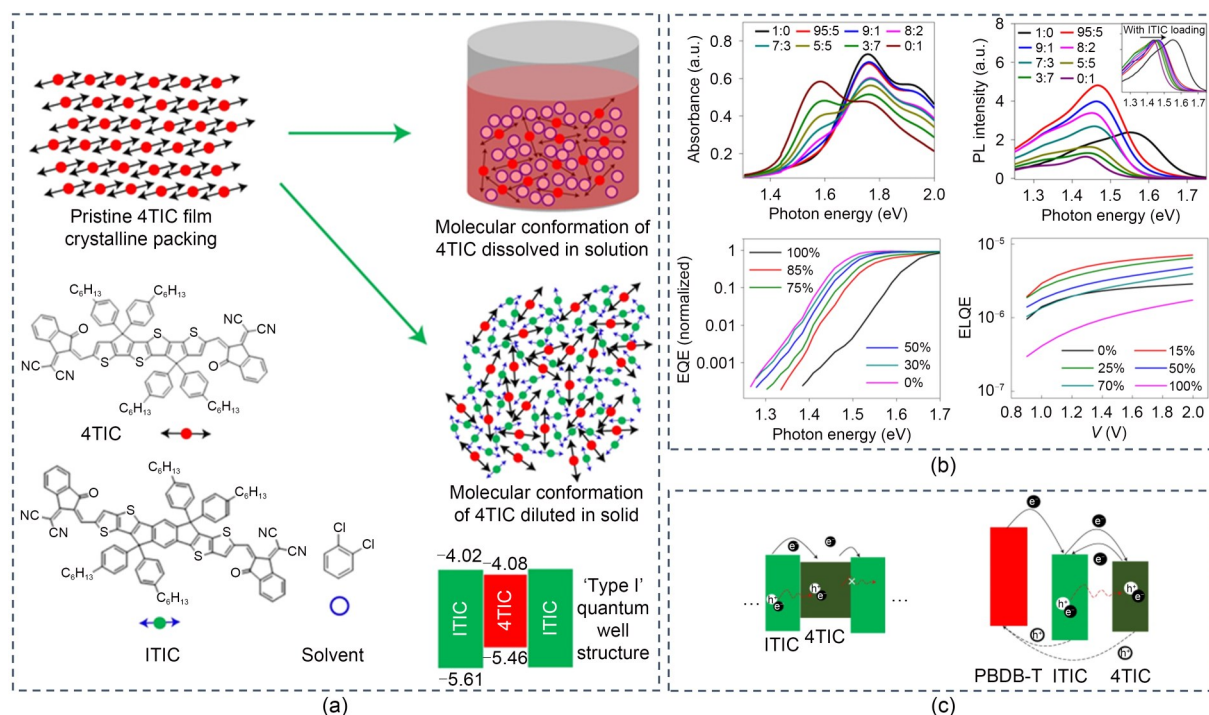


Fig. 1 (a) Schematic diagram of dilution effect, energy-level diagrams (unit: eV), molecular structures of ITIC and 4TIC, and dilution with solvent or solid; (b) Absorption spectra, PL spectra, EQE spectra, and ELQE curves of ITIC-4TIC at different weight ratios (V is the voltage); (c) Schematic diagrams for the charge and energy-transfer process between ITIC and 4TIC, and for charge and energy transfer in ternary blends. Reprinted from (Zuo et al., 2022), Copyright 2022, with permission from Springer Nature. References to color refer to the online version of this figure

mechanism is the hopping of the charges within the adjacent molecules. The LUMO offsets appear to affect composition-dependent carrier mobility.

With this understanding, we further outlined the material-selection rules for high-performance dilution-effect multi-component OPVs, which include: (1) good miscibility to facilitate molecular intermixing and enable the dilution effect to occur, (2) a larger band gap to ensure that the emission center is not changed and to form a lower local polarizability, (3) slightly higher LUMO levels to guarantee stability of the D:A charge-transfer center and efficient charge transport, and (4) lower local polarizability and/or formation of specific intermolecular packing structures to suppress the intramolecular bond vibrations that contribute to the molecular frontier orbitals. Then, we confirmed the generalizability of the dilution effect for enhancing the device performance of OPVs for a large range of NFA systems.

3.2 Effect of molecular packing

Although reduced electron-vibration coupling suppression has been confirmed in dilution-effect multi-component OPVs, it is still necessary to explore the

microscopic mechanism in order to develop appropriate materials that would minimize non-radiative charge recombination and enhance device efficiency. It is clear that the use of a larger band gap tends to form a low polarization environment to reduce electron-vibration coupling, but it remains unclear whether the molecular packing effect also matters. Indeed, adequate characterization of the molecular packing is quite challenging, because the active layer of OPVs is amorphous and understanding of electron vibration requires very detailed molecular packing information. Therefore, we used a molecular dynamic (MD) simulation to study the molecular packing in detail (Li et al., 2022). Based on the MD results, we verified the formation of molecular intermixing between the two NFAs; moreover, we saw that the end-group cyano indanone (IC) packing became more ordered in the blend film. An enhancement in molecular packing after blending in a third component has also been observed in other studies (Chen et al., 2023). Considering that the IC and thieno [3,2-*b*]thiophene (TT) connection is the most rotatable chemical bond, and contributes significantly to the frontier molecular orbitals, enhancement of IC packing

suppresses IC-TT-bond vibration. As a result, there is a significant enhancement in PL intensity after blending BTP-eC9 with BTP-S2, and the ELQE of the dilution-effect multi-component OPV increases dramatically (Li et al., 2022).

To further confirm the molecular packing effect on electron-vibration coupling in the NFA-based OPVs, we proposed a design with mutual dilution, which involved selecting two NFAs with similar band gaps, i.e. BTP-eC9 and BTP-S9, as shown in Fig. 2a (Zhan et al., 2022). The two molecules had almost identical optical properties and energetic structures, as well as polarizability. However, due to the use of extended conjugation at the end group, BTP-S9 exhibited better molecular packing behavior. Blending the two molecules together essentially excluded the effect of local polarizability on electron-vibration coupling, and allowed us to examine the molecular packing effect independently. We observed that the ternary OPV also exhibited improved ELQE and a lower V_{oc} loss. Significantly, the V_{oc} of the ternary OPV exhibited a convex composition-dependent behavior. This is actually hard to interpret with any existing working mechanism of ternary blends, but can be easily understood in terms of the dilution effect and molecular-packing-induced electron-vibration coupling suppression. Moreover, in the framework of the dilution effect, the variations in band gap and non-radiative charge recombination explain the composition-dependent V_{oc} behavior well for most ternary blends, as demonstrated in our previous work (Zuo et al., 2022). In addition, the blend film exhibited no blue shift in the absorption or PL spectra. On the contrary, the EQE response edge became sharper, suggesting that the blue shift in the blend mostly originated from the surrounding polarization effect (Liu et al., 2020).

Previous work has shown that substitution of a bromo group for a fluoro group can enhance intermolecular interaction. Inspired by this, we designed the BTP-H2 shown in Fig. 2b, in order to minimize electron-vibration coupling (He et al., 2022a). We identified the strong molecular packing of BTP-H2 via the grazing incidence wide-angle X-ray scattering (GIWAXS) method, and this significantly induced the spontaneous generation of delocalized excited species. A similar effect was observed when blending BTP-H2 with BTP-eC9. Due to the reduced non-radiative charge recombination, the V_{oc} loss of the ternary blend was

significantly reduced, and the best efficiency reached was 19.4%.

3.3 Extended strategies

In dilution-effect multi-component OPVs, the shrinkage of absorption spectra will cause a decrease in photo-current generation, primarily due to the surrounding polarization effect. To better balance photo-current generation and non-radiative V_{oc} loss, we propose a mixed diluent strategy, which involves one large-band gap diluent to tune the local polarizability and one low-band gap diluent to further increase intermolecular interactions, specifically IC-IC packing. We selected the BTP-S16 and BTP-S17 as the low-band gap and large-band gap NFAs, respectively, to “dilute” the BTP-eC9 in the PM6:BTP-eC9 blend (Chen et al., 2023). With this design, a better compromise between charge generation and charge recombination was achieved, which was validated by the high power conversion efficiencies (PCEs) achieved (up to 19.4%), as certified by the National PV Industry Measurement and Testing Center (NPVM), China. To the best of our knowledge, this result represents a record for certified single-junction OPVs.

Unlike the charge-recombination center in a pristine acceptor blend, that in an OPV is in the CT state, which involves a coulombically bounded hole-electron pair on both the donor and acceptor. As a result, the electron-vibration coupling in the OPV is from both the donor and the acceptor. Therefore, there is still plenty room to suppress the non-radiative charge recombination via diluting the donor component.

4 Multi-functional OPV devices

The most prominent advantage of OPVs lies in their multi-functionality: good semi-transparency, superior flexibility/stretchability, visual aesthetics, and other features that stem from the nature of organic semiconductors. Delicate design of the device structure and fundamental understanding of the optical and electrical processes are required to maximize overall performance.

4.1 Semitransparent OPVs

Solar energy consists of photons with different energies or wavelengths, and can be classified into the ultraviolet region, visible region, and infrared region.

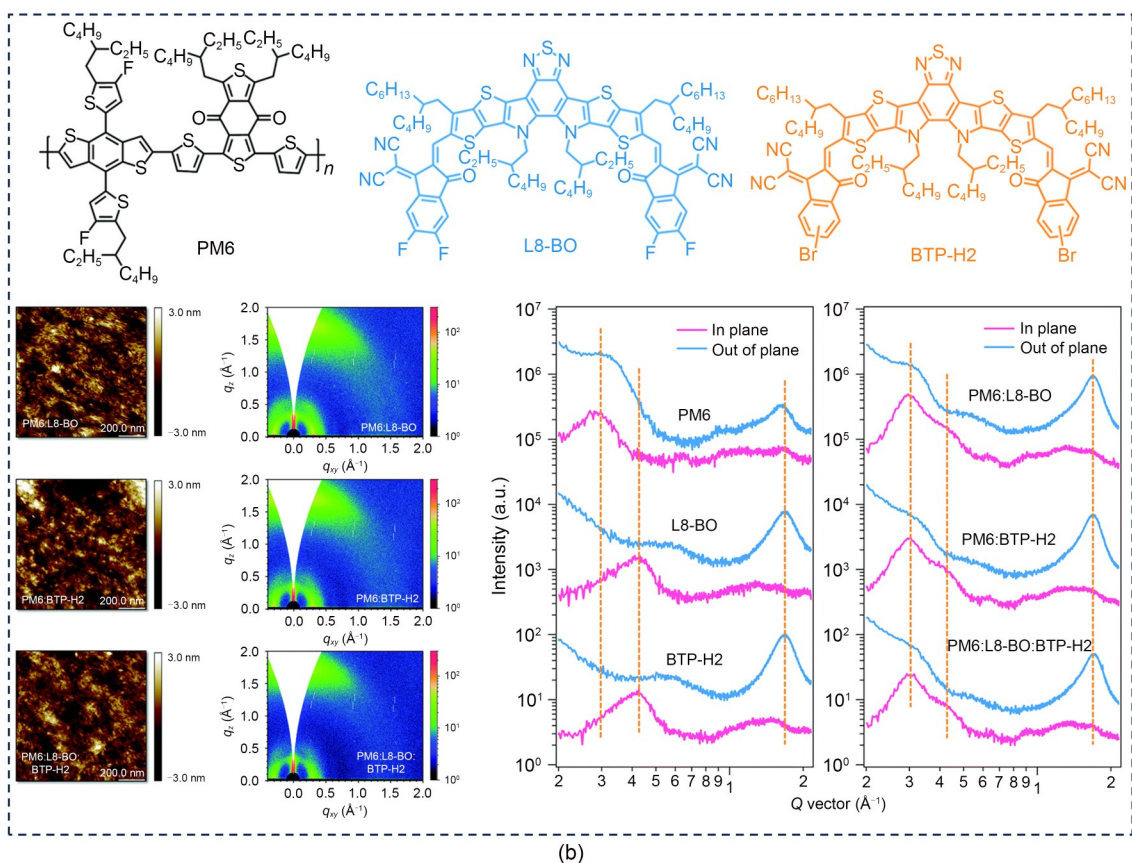
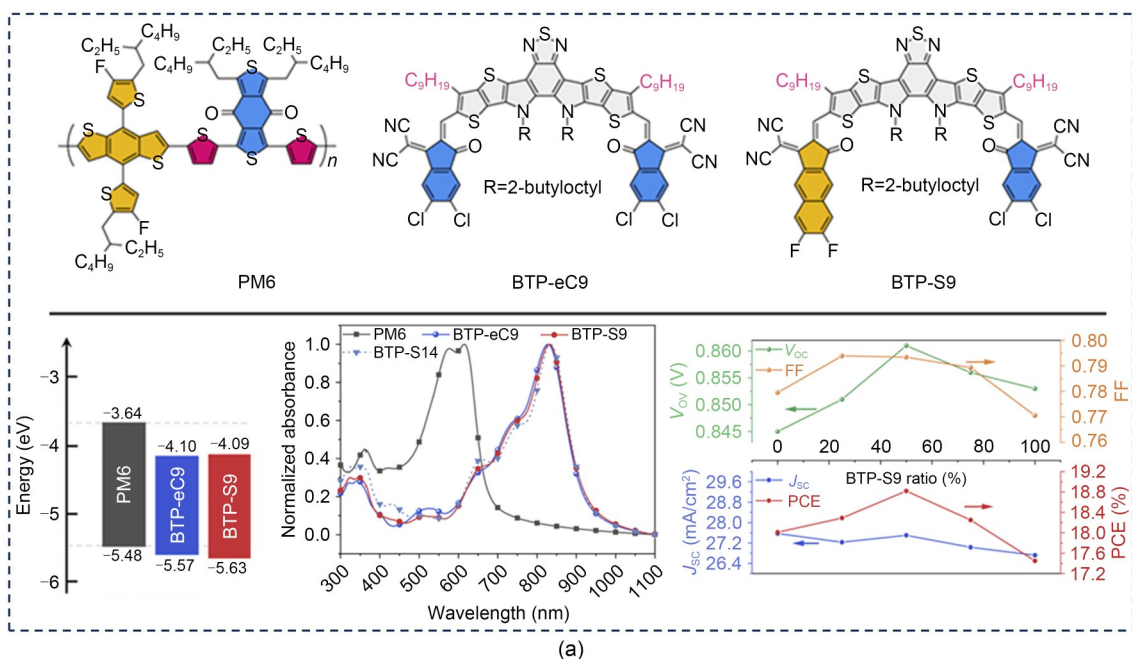


Fig. 2 (a) Chemical structures and properties of PM6, BTP-eC9, and BTP-S9, and the composition dependence of V_{oc} uplift in ternary devices (reprinted from (Zhan et al., 2022), Copyright 2022, with permission from Elsevier); (b) Chemical structures of PM6, L8-BO, and BTP-H2, and the results of GIWAXS testing (reprinted from (He et al., 2022b), Copyright 2022, with permission from RSC Publishing). J_{sc} is the short-circuit current density; q_z is the z-axis oriented scattering vector; q_{xy} is the scattering vector in the xy plane; Q is the scattering vector; L8-BO is the acceptor. References to color refer to the online version of this figure

It can be used for different purposes such as lighting, electricity generation, and temperature control (Singh et al., 2020). The semitransparent OPV (ST-OPV) was developed to comprehensively deliver the above functionalities, which can be widely applied in buildings or vehicles. It is clear that ST-OPVs should selectively absorb in the invisible ultraviolet and near infrared regions, transmit the visible photons, and reflect the middle/far infrared photons. However, the absorption coefficient of inorganic semiconductors increases monotonously with the photon energy, and this means its visible absorption will be much stronger if it absorbs in the infrared region (Lee et al., 2020). The absorption spectrum of organic semiconductors features tunable absorption peaks and valleys. It makes OPVs unique in their capacity for selective absorption, and especially suitable for ST-OPV applications (Chang et al., 2021; Xu et al., 2021; Liu et al., 2022; Zhang et al., 2022).

For ST-OPVs, it is clear that selective absorption is a key factor; it is a qualitative concept that offers intuitive understanding and guidance for material and

device structure design. In a recent paper, we proposed the numerical definition of the absorption selectivity (S), by simultaneously taking the invisible absorption and visible transmission into consideration (Li et al., 2021). This numerical definition provides quantitative understanding and guidance for ST-OPV. This parameter was found to directly correlate to light-utilization efficiency, which is a comprehensive parameter to evaluate the overall performance of ST-OPVs. This essentially guides us in material selection from a large pool of donor and acceptor materials, as well as in the optimization of device structures. For example, by analyzing the S values, we identified a combination of polymer donor PTB7-Th and NFA H3 as the most promising active layer, and selected it for ST-OPVs. We then optimized the interfacial properties of ultra-thin Ag and maximized the selective absorption via optical design. As a result, we developed a novel ST-OPV device structure with ultra-thin Ag capping and a TeO₂ anti-reflection layer, and achieved a high light-utilization efficiency of 4.0%, as shown in Fig. 3a.

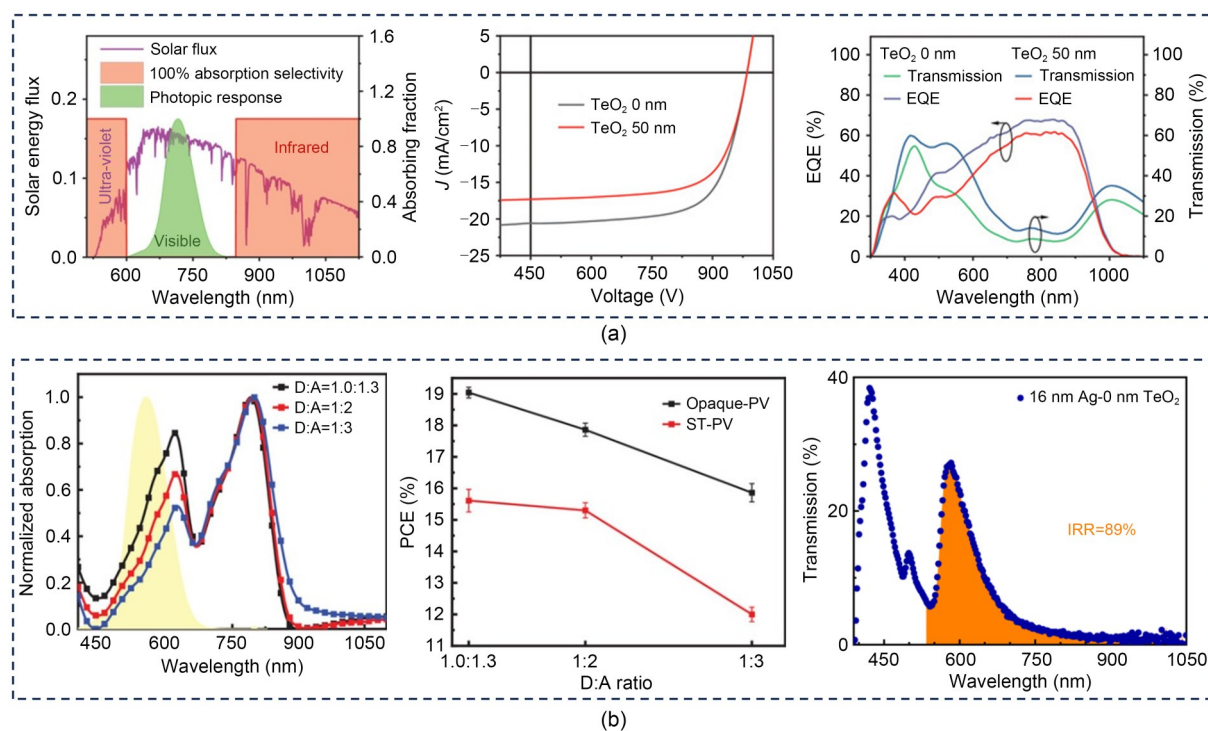


Fig. 3 (a) Solar flux, photopic response, and absorption profile of absolute absorption selectivity (absorption selectivity is 100%), J - V curves (J is the current density), EQE curves, and transmittance of ST-OPV without and with 50 nm TeO₂ (reprinted from (Li et al., 2021), Copyright 2021, with permission from John Wiley and Sons); (b) Normalized absorption spectra of PM6:L8-BO:BTP-eC9 blend films with different D:A weight ratios of 1.0:1.3, 1:2, and 1:3, with the yellow region representing the human eye's visible response, PCE dependence on the changing D:A weight ratios, and IRR of ST-OPV devices (reprinted from (Guan et al., 2022), Copyright 2022, with permission from John Wiley and Sons). References to color refer to the online version of this figure

An ST-OPV must convert enough photons into energy to qualify as a PV device. However, the above definition of S does not include the energy-conversion process. Therefore, we comprehensively incorporated energy conversion and selective absorption to optimize ST-OPVs. As shown in Fig. 3b, we used this logic to reappraise the strategies proposed to optimize the device performance of opaque OPVs in detail, including active-layer thickness, D:A ratios, and ultra-thin Ag film. As a result, we were able to further improve the light utilization efficiency (LUE) of ST-OPVs to over 5.0%, which is among the highest for ST-OPVs (Guan et al., 2022). We found that the device exhibited a good infrared-light rejection rate (IRR) of up to 89%, which is superior to commercial heat-insulation films such as 3M NV-25.

4.2 Flexible/stretchable OPVs

Organic semiconductors offer great advantages in terms of both optoelectronic properties and superior flexibility or stretchability. This is because they consist of intramolecular covalent bonds and intermolecular van der Waals interactions, which allow dislocation of molecules at no cost of defect formation under stress (Fukuda et al., 2020). In addition, organic molecules are soft, and can adapt to external stress by changing their conformation. However, advanced device structures are required to make OPVs flexible or stretchable. First, all layers (the substrate, interfacial layer, transparent electrode, and back electrode) need to be flexible. Second, the interface between each adjacent layer must be robust enough for bending or stretching cycles (Yang et al., 2021; Huang et al., 2023; Ye et al., 2023). The two major requirements cause the most critical challenges for flexible OPVs.

We previously demonstrated that the ultra-Ag-based top-illumination (TUA) device structure is promising for flexible OPV application (Zuo et al., 2014). Different to previous designs in which the light penetrates from the substrate, the TUA structure consists of an electrode on the substrate, interfacial layer, active layer, interfacial layer, ultra-thin Ag layer, and top optical capping layer, sequentially, and thus it allows the light to reach the device directly without penetrating the substrate. This structure allows ease of integration with the substrate, good flexibility, low-cost production, and good scalability. Moreover, it enables a device performance of over 7% on both flexible and rigid substrates,

which is quite good (Zhao et al., 2021). Taking advantage of recent advancements in NFA materials, we also fabricated high-performance flexible OPVs based on the TUA device structure, which exhibited a certified efficiency of 12% (Zhao et al., 2022). By tailoring the interfacial contact properties using the p-type conductive polymer PCP-Li as the bridging layer, we successfully deposited aqueous poly(3,4-ethylenedioxythiophene):poly(styrenesulfonate) (PEDOT:PSS) on the thick Ag layer. This allowed us to reach an even higher efficiency of 16% (Zheng et al., 2022). We improved the ultra-thin Ag film quality via the wetting method, and further enhanced device efficiency to over 17%, which represents the best among flexible OPVs (Zheng et al., 2023). The device also showed hardly any change in efficiency after bending 10000 times with a radius of 4 mm. In addition, we found that up-scaling the device area from 0.1 to 1.0 cm² caused no loss in efficiency, and device color could be easily tuned by simply adjusting the capping layer, as shown in Fig. 4a. Aside from the intrinsic factors, OPV flexibility is also related to the geometry factor, with thinner devices delivering better flexibility. Without a substrate, the thickness of a TUA device is around 300 nm, which is very flexible. However, fabricating “free-standing” high-performance OPVs or integrating them with ultra-thin substrates is quite challenging. An advantage of the TUA device is that it can be easily integrated with a variety of substrates, regardless of its optical transparency and film thickness. Therefore, we tried integrating the device on a 1.2- μ m polyimide substrate, and found that the device’s performance was very similar to that on a glass substrate. However, this ultra-thin OPV had different mechanical properties. First, it exhibited a very high specific power density of 40 W/g. Second, such a thin device makes a small bump when compressed, which allows for pseudo-stretchability. Third, this device was adaptable to most non-planar surfaces, and easy to integrate with most surfaces, including human skin.

Bending the device exerts a combination of stretching and compressing, but with a low strain (about 1%). Furthermore, stretchable OPVs must undergo a large strain of over 10%, which means more harsh requirements on materials and devices. Thereafter, the stretchable OPV can be applied in more diverse scenarios compared to flexible ones. We took on this challenge by expanding the TUA structure of the substrate, back electrode, active layer, and top electrode. As shown in

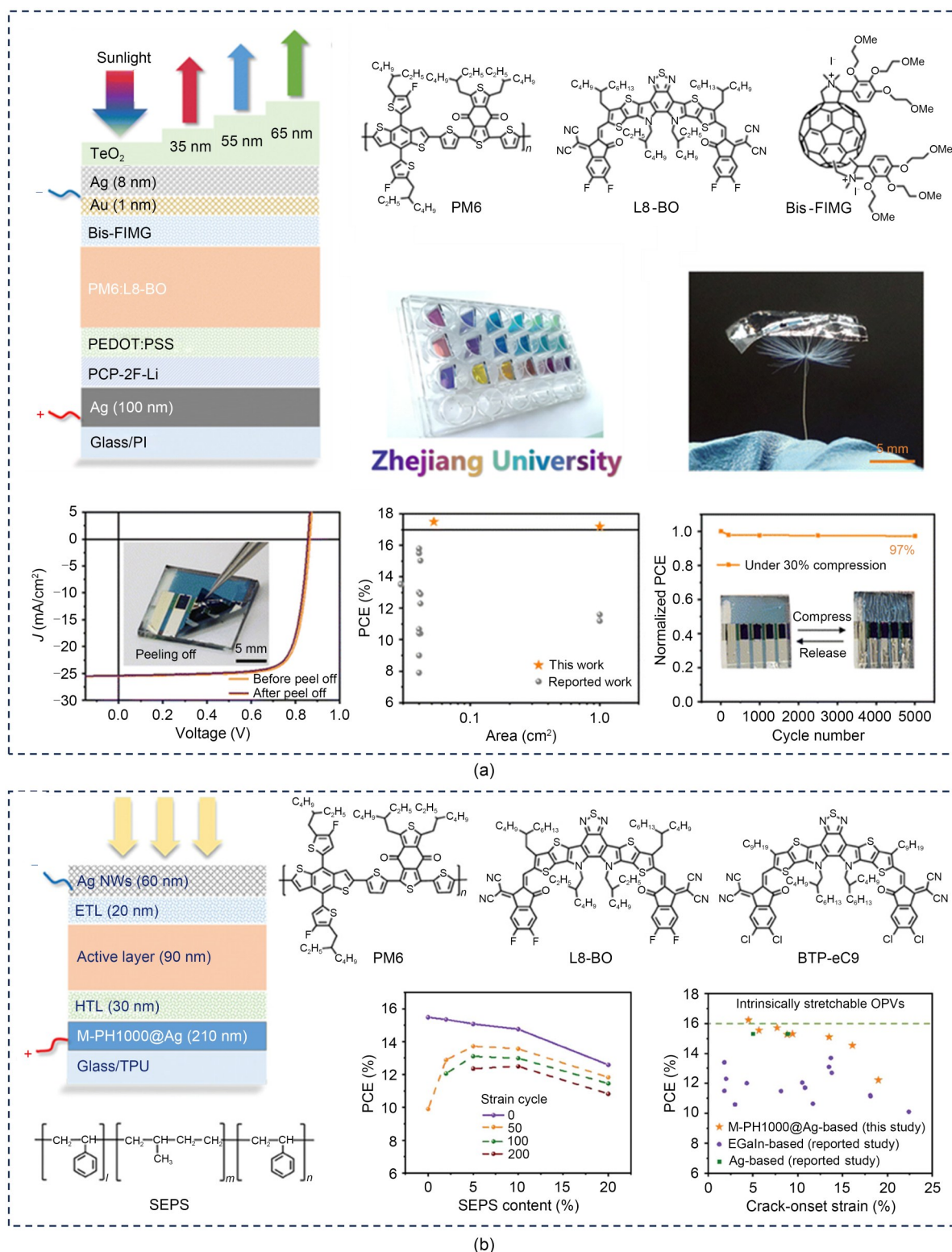


Fig. 4 (a) Structure and performance of an ultra-thin OPV with a power density of nearly 40 W/g (reprinted from (Zheng et al., 2023), Copyright 2023, with permission from RSC Publishing); (b) Structure and performance of an intrinsically stretchable OPV (reprinted from (Zheng et al., 2014), Copyright 2014, with permission from John Wiley and Sons). Bis-FIMG is the bisfulleropyrrolidine-tris(methoxyethoxy)phenyl; NW is the nanowire; ETL is the electron transport layer; HTL is the hole transport layer; TPU is the thermoplastic urethane. References to color refer to the online version of this figure

Fig. 4b, we used a polyurethane elastomer as the substrate; the back electrode consisted of PEDOT:PSS and Ag composites, and an elastic polymer (SEPS) was blended with the active layer to enhance its stretchability. Ag nanowires were used as a stretchable transparent electrode for ultra-thin Ag replacement (Zheng et al., 2024). As a result, we achieved record-breaking efficiency of 16.23%, and after stretching for 200 cycles with a strain of 10%, the device retained 80% of the efficiency before stretching.

5 Summary

In the past three years, our group has focused on addressing the V_{oc} loss issue in OPVs, and successfully reduced the non-radiative charge recombination induced by electron-vibration coupling by tailoring intermolecular interaction. In particular, we propose using the dilution effect in producing multi-component OPVs, which inspires the general material-selection rule for high-performance OPVs. We also unveil the details underlying the local polarizability effect and molecular packing effect. We have made efforts to improve the performance of multi-functional OPVs, including semitransparent devices and flexible/stretchable devices. Based on a fundamental understanding of the optical, electrical, thermal, and mechanical properties of OPVs, we propose the concept of absorption selectivity, and have designed novel devices that offer more and better functionalities.

Acknowledgments

This work is supported by the National Natural Science Foundation of China (Nos. 52173185 and 52127806) and the National Key Research and Development Program of China (No. 2022YFB4200600). Lijian ZUO thanks the Research Start-up Fund from Zhejiang University.

Author contributions

Yiming WANG and Lijian ZUO wrote and revised the manuscript.

Conflict of interest

Yiming WANG and Lijian ZUO declare that they have no conflict of interest.

References

Amirkhani S, Bahadori-Jahromi A, Mylona A, et al., 2019. Impact of Low-E window films on energy consumption

- and CO₂ emissions of an existing UK hotel building. *Sustainability*, 11(16):4265.
<https://doi.org/10.3390/su11164265>
- Benduhn J, Tvingstedt K, Piersimoni F, et al., 2017. Intrinsic non-radiative voltage losses in fullerene-based organic solar cells. *Nature Energy*, 2(6):17053.
<https://doi.org/10.1038/nenergy.2017.53>
- Bulović V, Deshpande R, Thompson ME, et al., 1999. Tuning the color emission of thin film molecular organic light emitting devices by the solid state solvation effect. *Chemical Physics Letters*, 308(3-4):317-322.
[https://doi.org/10.1016/S0009-2614\(99\)00580-1](https://doi.org/10.1016/S0009-2614(99)00580-1)
- Bulović V, Shoustikov A, Baldo MA, et al., 1998. Bright, saturated, red-to-yellow organic light-emitting devices based on polarization-induced spectral shifts. *Chemical Physics Letters*, 287(3-4):455-460.
[https://doi.org/10.1016/S0009-2614\(98\)00168-7](https://doi.org/10.1016/S0009-2614(98)00168-7)
- Chang YL, Zhu XW, Zhu LY, et al., 2021. Regioregular narrow bandgap copolymer with strong aggregation ability for high-performance semitransparent photovoltaics. *Nano Energy*, 86:106098.
<https://doi.org/10.1016/j.nanoen.2021.106098>
- Chen TY, Li SX, Li YK, et al., 2023. Compromising charge generation and recombination of organic photovoltaics with mixed diluent strategy for certified 19.4% efficiency. *Advanced Materials*, 35(21):e2300400.
<https://doi.org/10.1002/adma.202300400>
- Datt R, Lee HKH, Zhang GC, et al., 2022. Organic solar cells at stratospheric condition for high altitude platform station application. *Chinese Journal of Chemistry*, 40(24):2927-2932.
<https://doi.org/10.1002/cjoc.202200481>
- de Jong M, Seijo L, Meijerink A, et al., 2015. Resolving the ambiguity in the relation between Stokes shift and Huang-Rhys parameter. *Physical Chemistry Chemical Physics*, 17(26):16959-16969.
<https://doi.org/10.1039/C5CP02093J>
- Fukuda K, Yu K, Someya T, 2020. The future of flexible organic solar cells. *Advanced Energy Materials*, 10(25):2000765.
<https://doi.org/10.1002/aenm.202000765>
- Guan ST, Li YK, Yan KR, et al., 2022. Balancing the selective absorption and photon-to-electron conversion for semitransparent organic photovoltaics with 5.0% light-utilization efficiency. *Advanced Materials*, 34(41):2205844.
<https://doi.org/10.1002/adma.202205844>
- Günther M, Kazerouni N, Blätte D, et al., 2023. Models and mechanisms of ternary organic solar cells. *Nature Reviews Materials*, 8(7):456-471.
<https://doi.org/10.1038/s41578-023-00545-1>
- He CL, Chen Z, Wang TH, et al., 2022a. Asymmetric electron acceptor enables highly luminescent organic solar cells with certified efficiency over 18%. *Nature Communications*, 13(1):2598.
<https://doi.org/10.1038/s41467-022-30225-7>
- He CL, Pan YW, Ouyang YN, et al., 2022b. Manipulating the D:A interfacial energetics and intermolecular packing for 19.2% efficiency organic photovoltaics. *Energy & Environmental Science*, 15(6):2537-2544.

- <https://doi.org/10.1039/D2EE00595F>
- Hong YN, Lam JWY, Tang BZ, 2009. Aggregation-induced emission: phenomenon, mechanism and applications. *Chemical Communications*, (29):4332-4353. <https://doi.org/10.1039/B904665H>
- Hong YN, Lam JWY, Tang BZ, 2011. Aggregation-induced emission. *Chemical Society Reviews*, 40(11):5361-5388. <https://doi.org/10.1039/C1CS15113D>
- Huang JM, Lu Z, He JQ, et al., 2023. Intrinsically stretchable, semi-transparent organic photovoltaics with high efficiency and mechanical robustness via a full-solution process. *Energy & Environmental Science*, 16(3):1251-1263. <https://doi.org/10.1039/D2EE03096A>
- Huang Y, Kramer EJ, Heeger AJ, et al., 2014. Bulk heterojunction solar cells: morphology and performance relationships. *Chemical Reviews*, 114(14):7006-7043. <https://doi.org/10.1021/cr400353v>
- Kumar A, Devine R, Mayberry C, et al., 2010. Origin of radiation-induced degradation in polymer solar cells. *Advanced Functional Materials*, 20(16):2729-2736. <https://doi.org/10.1002/adfm.201000374>
- Lee K, Kim N, Kim K, et al., 2020. Neutral-colored transparent crystalline silicon photovoltaics. *Joule*, 4(1):235-246. <https://doi.org/10.1016/j.joule.2019.11.008>
- Li YK, Guo Y, Chen Z, et al., 2022. Mechanism study on organic ternary photovoltaics with 18.3% certified efficiency: from molecule to device. *Energy & Environmental Science*, 15(2):855-865. <https://doi.org/10.1039/D1EE02977K>
- Li YK, He CL, Zuo LJ, et al., 2021. High-performance semi-transparent organic photovoltaic devices via improving absorbing selectivity. *Advanced Energy Materials*, 11(11):2003408. <https://doi.org/10.1002/aenm.202003408>
- Lim DH, Ha JW, Choi H, et al., 2021. Recent progress of ultra-narrow-bandgap polymer donors for NIR-absorbing organic solar cells. *Nanoscale Advances*, 3(15):4306-4320. <https://doi.org/10.1039/D1NA00245G>
- Liu S, Yuan J, Deng WY, et al., 2020. High-efficiency organic solar cells with low non-radiative recombination loss and low energetic disorder. *Nature Photonics*, 14(5):300-305. <https://doi.org/10.1038/s41566-019-0573-5>
- Liu X, Zhong ZP, Zhu RH, et al., 2022. Aperiodic band-pass electrode enables record-performance transparent organic photovoltaics. *Joule*, 6(8):1918-1930. <https://doi.org/10.1016/j.joule.2022.06.009>
- Liu Y, Zuo LJ, Shi XL, et al., 2018. Unexpectedly slow yet efficient picosecond to nanosecond photoinduced hole-transfer occurs in a polymer/nonfullerene acceptor organic photovoltaic blend. *ACS Energy Letters*, 3(10):2396-2403. <https://doi.org/10.1021/acsenenergylett.8b01416>
- Maka AOM, Alabid JM, 2022. Solar energy technology and its roles in sustainable development. *Clean Energy*, 6(3):476-483. <https://doi.org/10.1093/ce/zkac023>
- Northey T, Stacey J, Penfold TJ, 2017. The role of solid state solvation on the charge transfer state of a thermally activated delayed fluorescence emitter. *Journal of Materials Chemistry C*, 5(42):11001-11009. <https://doi.org/10.1039/C7TC04099G>
- Park SH, Roy A, Beaupré S, et al., 2009. Bulk heterojunction solar cells with internal quantum efficiency approaching 100%. *Nature Photonics*, 3(5):297-302. <https://doi.org/10.1038/nphoton.2009.69>
- Scharber MC, Sariciftci NS, 2021. Low band gap conjugated semiconducting polymers. *Advanced Materials Technologies*, 6(4):2000857. <https://doi.org/10.1002/admt.202000857>
- Shi XL, Zuo LJ, Jo SB, et al., 2017. Design of a highly crystalline low-band gap fused-ring electron acceptor for high-efficiency solar cells with low energy loss. *Chemistry of Materials*, 29(19):8369-8376. <https://doi.org/10.1021/acs.chemmater.7b02853>
- Singh V, Rayal I, Priyanaka, et al., 2020. Chapter 1—solar radiation and light materials interaction. In: Dalapati GK, Sharma M (Eds.), *Energy Saving Coating Materials*. Elsevier, p.1-32. <https://doi.org/10.1016/B978-0-12-822103-7.00001-7>
- Tak S, Woo S, Park J, et al., 2017. Effect of the changeable organic semi-transparent solar cell window on building energy efficiency and user comfort. *Sustainability*, 9(6):950. <https://doi.org/10.3390/su9060950>
- Traverse CJ, Pandey R, Barr MC, et al., 2017. Emergence of highly transparent photovoltaics for distributed applications. *Nature Energy*, 2(11):849-860. <https://doi.org/10.1038/s41560-017-0016-9>
- Vandewal K, Tvingstedt K, Gadisa A, et al., 2009. On the origin of the open-circuit voltage of polymer–fullerene solar cells. *Nature Materials*, 8(11):904-909. <https://doi.org/10.1038/nmat2548>
- Veldman D, İpek Ö, Meskers SCJ, et al., 2008. Compositional and electric field dependence of the dissociation of charge transfer excitons in alternating polyfluorene copolymer/fullerene blends. *Journal of the American Chemical Society*, 130(24):7721-7735. <https://doi.org/10.1021/ja8012598>
- Victoria M, Haegel N, Peters IM, et al., 2021. Solar photovoltaics is ready to power a sustainable future. *Joule*, 5(5):1041-1056. <https://doi.org/10.1016/j.joule.2021.03.005>
- Wang D, Liu HR, Li YH, et al., 2021. High-performance and eco-friendly semitransparent organic solar cells for greenhouse applications. *Joule*, 5(4):945-957. <https://doi.org/10.1016/j.joule.2021.02.010>
- Wang YM, Yu JW, Zhang R, et al., 2023. Origins of the open-circuit voltage in ternary organic solar cells and design rules for minimized voltage losses. *Nature Energy*, 8(9):978-988. <https://doi.org/10.1038/s41560-023-01309-5>
- Xu CY, Jin K, Xiao Z, et al., 2021. Wide bandgap polymer with narrow photon harvesting in visible light range enables efficient semitransparent organic photovoltaics. *Advanced Functional Materials*, 31(52):2107934. <https://doi.org/10.1002/adfm.202107934>
- Yang F, Huang YT, Li YW, et al., 2021. Large-area flexible organic solar cells. *npj Flexible Electronics*, 5(1):30.

- <https://doi.org/10.1038/s41528-021-00128-6>
- Ye QR, Chen ZY, Yang DB, et al., 2023. Ductile oligomeric acceptor-modified flexible organic solar cells show excellent mechanical robustness and near 18% efficiency. *Advanced Materials*, 35(44):2305562. <https://doi.org/10.1002/adma.202305562>
- Yuan YB, Reece TJ, Sharma P, et al., 2011. Efficiency enhancement in organic solar cells with ferroelectric polymers. *Nature Materials*, 10(4):296-302. <https://doi.org/10.1038/nmat2951>
- Zhan LL, Li SX, Li YK, et al., 2022. Desired open-circuit voltage increase enables efficiencies approaching 19% in symmetric-asymmetric molecule ternary organic photovoltaics. *Joule*, 6(3):662-675. <https://doi.org/10.1016/j.joule.2022.02.001>
- Zhang HT, Tian P, Zhong J, et al., 2023. Mapping photovoltaic panels in coastal China using Sentinel-1 and Sentinel-2 images and Google Earth Engine. *Remote Sensing*, 15(15):3712. <https://doi.org/10.3390/rs15153712>
- Zhang YN, Luo D, Shan CW, et al., 2022. High-performance semitransparent organic solar cells enabled by improved charge transport and optical engineering of ternary blend active layer. *Solar RRL*, 6(1):2100785. <https://doi.org/10.1002/solr.202100785>
- Zhang ZX, Chen M, Zhong T, et al., 2023. Carbon mitigation potential afforded by rooftop photovoltaic in China. *Nature Communications*, 14(1):2347. <https://doi.org/10.1038/s41467-023-38079-3>
- Zhao F, Zuo LJ, Li YK, et al., 2021. High-performance upscaled indium tin oxide-free organic solar cells with visual esthetics and flexibility. *Solar RRL*, 5(9):2100339. <https://doi.org/10.1002/solr.202100339>
- Zhao F, Zheng XJ, Li SX, et al., 2022. Non-halogenated solvents processed efficient ITO-free flexible organic solar cells with upscaled area. *Macromolecular Rapid Communications*, 43(16):2200049. <https://doi.org/10.1002/marc.202200049>
- Zheng XJ, Zuo LJ, Zhao F, et al., 2022. High-efficiency ITO-free organic photovoltaics with superior flexibility and upscalability. *Advanced Materials*, 34(17):2200044. <https://doi.org/10.1002/adma.202200044>
- Zheng XJ, Zuo LJ, Yan KR, et al., 2023. Versatile organic photovoltaics with a power density of nearly 40 W g⁻¹. *Energy & Environmental Science*, 16(5):2284-2294. <https://doi.org/10.1039/D3EE00087G>
- Zheng XJ, Wu XL, Wu Q, et al., 2024. Thorough optimization for intrinsically stretchable organic photovoltaics. *Advanced Materials*, 36(11):2307280. <https://doi.org/10.1002/adma.202307280>
- Zhong Q, Nelson JR, Tong DQ, et al., 2022. A spatial optimization approach to increase the accuracy of rooftop solar energy assessments. *Applied Energy*, 316:119128. <https://doi.org/10.1016/j.apenergy.2022.119128>
- Zuo LJ, Chueh CC, Xu YX, et al., 2014. Microcavity-enhanced light-trapping for highly efficient organic parallel tandem solar cells. *Advanced Materials*, 26(39):6778-6784. <https://doi.org/10.1002/adma.201402782>
- Zuo LJ, Jo SB, Li YK, et al., 2022. Dilution effect for highly efficient multiple-component organic solar cells. *Nature Nanotechnology*, 17(1):53-60. <https://doi.org/10.1038/s41565-021-01011-1>